Krebs, H., Schmid, F. X., & Jaenicke, R. (1983) *J. Mol. Biol. 169*, 619–635.
Krebs, H., Schmid, F. X., & Jaenicke, R. (1985) *Biochemistry 24*, 3846–3852.
Lin, L.-N., & Brandts, J. F. (1983a) *Biochemistry 22*, 559–563.
Lin, L.-N., & Brandts, J. F. (1983b) *Biochemistry 22*, 564–573.
Lin, L.-N., & Brandts, J. F. (1983c) *Biochemistry 22*, 573–580.
Matheson, R. R., Jr., & Scheraga, H. A. (1979) *Biochemistry 18*, 2437–2445.
Mui, P. W., Konishi, Y., & Scheraga, H. A. (1985) *Biochemistry 24*, 4481–4489.
Nall, B. T., Garel, J., & Baldwin, R. L. (1978) *J. Mol. Biol. 118*, 317–330.
Schmid, F. X. (1983) *Biochemistry 22*, 4690–4696.
Schmid, F. X., & Baldwin, R. L. (1979) *J. Mol. Biol. 135*, 199–215.
Schmid, F. X., & Blascheck, H. A. (1981) *Eur. J. Biochem. 114*, 111–117.
Schmid, F. X., Grafl, R., Wrba, A., & Beintema, J. J. (1986) *Proc. Natl. Acad. Sci. U.S.A. 83*, 872–876.

Intermediates in the Refolding of Ribonuclease at Subzero Temperatures. 3. Multiple Folding Pathways†

Roger G. Biringer‡ and Anthony L. Fink*
Department of Chemistry, The University of California, Santa Cruz, California 95064
Received September 29, 1986; Revised Manuscript Received July 13, 1987

ABSTRACT: The kinetics of refolding of ribonuclease A have been measured at −15 °C by monitoring the intrinsic fluorescence and absorbance signals from the six tyrosine residues. For each probe multiphasic kinetics were observed. The burial of tyrosine residues, as determined by the change in absorbance at 286 nm, revealed four phases, whereas the kinetics of refolding monitored by fluorescence revealed only two phases. The rates of the transients detected by fluorescence were independent of pH. One of the faster transients detected by ΔA_{286} involved a decrease in absorbance, which is consistent with solvent exposure, rather than burial, and suggests the possibility of an abortive partially folded intermediate in the earlier stages of folding. Double-jump unfolding assays were used to follow the buildup and decay of an intermediate in the refolding reaction at −15 °C. At both pH* 3.0 and pH* 6.0 the maximum concentration of the intermediate was 25–30% of the total protein. The existence of a second pathway of slow folding was inferred from the difference in rate of formation of native enzyme and breakdown of the observed intermediate, and by computer simulations. In addition, the unfolding assay demonstrated that 20% of the unfolded protein was converted to native at a much faster rate, consistent with observations in aqueous solution that 80% of unfolded ribonuclease A consists of slow-folding species. Kinetics and amplitude data from these and other refolding experiments with different probes were used to develop possible models for the pathway of refolding. The simplest system consistent with the results for the slow-refolding species involves two parallel pathways with multiple intermediates on each of them. Several independent lines of evidence indicate that about 30% of the unfolded state refolds by the minor pathway, in which the slowest observed phase is attributed to the isomerization of Pro-93. The major pathway involves 50% of the unfolded state; the reason why it refolds slowly is not apparent. A native-like intermediate is formed considerably more rapidly in the major slow-refolding pathway, compared to the minor pathway.

Preliminary experiments (Biringer & Fink, 1982a,b, 1988; Fink, 1986; Fink & Painter, 1987) have indicated that investigation of the folding of proteins in aqueous methanol cryosolvents at subzero temperatures may provide an important new method for determination of the pathway of protein folding. In particular, this approach facilitates the stabilization of partially folded states with exposed hydrophobic surfaces. By monitoring probes reflecting the state (native or solvent exposed) of different regions of the molecule, it is possible to map out the details of the folding pathway.

The work reported herein is a continuation of our studies on the folding of ribonuclease A. Complications exist since unfolded ribonuclease is a mixture of slow (U_S)[1] and fast (U_F) folding species (Garel & Baldwin, 1973). The fast-refolding molecules constitute 20% of the total in aqueous solution, and the remaining slow-folding molecules are of at least two distinct types (Schmid & Blascheck, 1981). It was first proposed by Brandts et al. (1975) that the slow-folding molecules differ from the fast-folding ones by virtue of proline cis/trans isomerization.

There have been several reports that an intermediate with properties very similar to native RNase is formed during the folding under native conditions (Kim & Baldwin, 1982; Cook

† This research was supported by grants from the National Science Foundation.
‡ Present address: Department of Chemistry, San Jose State University, San Jose, CA 95192.

[1] Abbreviations: RNase, ribonuclease A; proton NMR, proton nuclear magnetic resonance; pH*, apparent pH of mixed aqueous–organic solvent; U, unfolded state; N, native state; nitro-Tyr-115, derivative of ribonuclease A in which Tyr-115 has been nitrated; Gdn·HCl, guanidine hydrochloride; ΔF, change in fluorescence; IEF, isoelectric focusing.

0006-2960/88/0427-0315$01.50/0

et al., 1979; Schmid & Blascheck, 1981). Schmid (1983) found that although this intermediate is similar to native RNase A it unfolded at a faster rate in guanidine hydrochloride than the native protein. He exploited this phenomenon to measure the concentration of this intermediate during the folding process. Aliquots taken at early times in the folding produced biphasic unfolding kinetics, the faster phase corresponding to the unfolding of the intermediate and the slower to that of the native. When the amplitudes of each phase were plotted as a function of folding time, the data revealed that the concentration of the intermediate proceeded through a maximum and there was a lag in the formation of native material. Kinetic analysis showed that the intermediate was formed at a rate faster than that for the native state and decayed with a rate equivalent to that for the formation of native protein. The interpretation of these findings is that the two processes are directly coupled. Further, the rates obtained from these experiments compare well with those obtained from UV absorption and fluorescence experiments. In addition, the rate corresponding to the decay of the intermediate is that which has been unambiguously shown to represent a proline isomerization process (Lin & Brandts, 1983b).

In this report we have used the intrinsic fluorescence and absorbance signals from the six tyrosine residues of RNase A to monitor the refolding process in methanol cryosolvents at −15 °C. We also present the results of double-jump unfolding assays of RNase A unfolded in aqueous methanol and refolded in 35% methanol at −15 °C. In addition, the results from unfolding kinetics studies in the two preceding papers in this issue (Biringer & Fink, 1988; Biringer et al., 1988) are analyzed in the context of the unfolding assay data to produce a model for the refolding of ribonuclease.

Experimental Procedures

Ribonuclease A (Calbiochem) was purified as described previously (Biringer & Fink, 1982a, 1988). Reduction and carboxymethylation of ribonuclease A was accomplished according to the procedure of Takahashi et al. (1977). Other materials used are described in the preceding papers (Biringer & Fink, 1988; Biringer et al., 1988).

Refolding Monitored by Absorbance. Absorbance measurements of folding were performed at 286 nm on a Cary 118 spectrophotometer. An insulated, thermostated brass-block cell holder was used to maintain constant temperature in the sample cuvette. Cooling was provided by either a Neslab RTE-8 or RTE-4 bath. The cell compartment was constantly purged with either dry nitrogen or air which had been dried by a molecular sieve drying apparatus (Wilkerson Corp.). Temperature was monitored with a BAT-12 electronic thermometer (Sensortek Inc.). The probe was attached to the outside of the cuvette.

In a typical refolding experiment, a 20–60-μL aliquot of concentrated protein solution (pH* 3, 35% methanol) was taken up into a gas-tight microsyringe (Hamilton) and incubated for 10 min at 70 °C in a water bath. Previous experiments using NMR had demonstrated that these conditions result in the apparent complete unfolding of RNase (Biringer & Fink, 1982a). The syringe contents were then injected into a thermostated cuvette containing 1.0 mL of cryosolvent held at −15 ± 0.2 °C. Immediately after injection, the solution was mixed with a *precooled*, vibrating plumper (Calbiochem) for 20–30 s. The time-dependent changes in the absorbance or fluorescence were directly accumulated on a microcomputer interfaced to the spectrophotometer. By appropriate signal averaging the sensitivity of the instrument was significantly increased. In some experiments the protein was unfolded in 5 M Gdn·HCl, pH 2, for 30 min.

The enzyme concentrations and solvent composition varied with the particular experiment. Stock solutions were 0.35–0.75 mM protein, pH* 3.0, and 0.033 M sodium formate in 35% methanol.

Comparison of the absorption spectra of native RNase A to that of guanidine-unfolded or thermally unfolded protein reveals a range of wavelengths (250–260 nm) in which the absorbances are identical. The region has also been observed in aqueous spectra (Garel et al., 1976; Nall et al., 1978). Since the signal in this region is independent of protein conformation, any change observed in this region during the folding process must be due to processes other than folding. The folding of RNase was followed at the center of this region (254 nm) at both pH* 3.0 and pH* 6.0 as a control to monitor for aggregation or other artifacts. In all cases the signal remained constant throughout the time course of the folding process. Aggregation could be induced by refolding protein that had been stored at room temperature for over 1 week in 35% methanol. Refolding of such solutions produced large changes in absorbance at 254 nm and thus proved the validity of the technique. Second, the time course of the change is at least an order of magnitude greater than the reported folding process. In all other refolding experiments stock protein solutions were either prepared fresh or used within a day after storage at 0 °C or below. Thus all the tests for the presence of aggregation during refolding were negative.

Reversible Thermal Unfolding. The reversible unfolding of RNase in 35% methanol was monitored at pH* 3.0 and 6.0 by absorbance change at 286 nm, and by fluorescence change at 305 nm (excitation at 289 nm). The procedures used have been described previously (Biringer & Fink, 1988).

Experiments To Detect Deamidation. Ribonuclease was tested for the presence of thermally induced deamidation under each set of conditions employed in the thermal denaturation studies. An aliquot was taken from the sample solution after completion of the unfolding (or refolding) transition and subjected to analytical IEF, pH 3–10 range.

Fluorescence Measurements. Fluorescence measurements of the folding were performed with a Perkin-Elmer MPF-4 spectrofluorometer with the excitation wavelength set at 280 nm (slit = 2 nm) and the emission at 305 nm (slit = 6 nm). All other conditions and methods were identical with those of the absorbance studies except that the stock enzyme concentration was 0.75 mM.

Control Experiments. Most of these have been discussed in a preceding paper (Biringer & Fink, 1988). The addition of solutions of Gdn·HCl-unfolded ribonuclease to the cryosolvent at −15 °C requires a significant time period for complete mixing and equilibration. Consequently, for pragmatic reasons we usually used thermally unfolded protein. However, a number of refolding kinetics experiments were performed with protein samples that were unfolded in 5 M Gdn·HCl. For example, by use of fluorescence to monitor the refolding at both pH* 3 and pH* 6, the kinetics were same, within experimental error, as those observed with thermally unfolded protein [see inset to Figure 4B and also Table V in Biringer and Fink (1988)]. The amplitudes of each of the two phases were 2–4% larger in the case of the Gdn·HCl-unfolded samples. Similarly, when the absorbance at 286 nm was used to monitor the refolding reaction, similar rates and amplitudes to those found with thermally unfolded protein were observed.

Amplitude Calculations. The amplitudes for each set of folding experiments monitored by both absorbance and fluorescence were standardized to the difference between native

and unfolded protein. Two methods were used to determine the total amplitude for the folding process: unfolding in 5 M guanidine hydrochloride and thermal unfolding. In the latter case, the temperature effect on the extinction of the tyrosine residues plays a major part in determining the amplitude. *N*-Acetyltyrosine ethyl ester was used as a model for exposed tyrosines. The absorbance of this compound decreases linearly as a function of temperature. The theoretical amplitude for folding was assumed to be the sum of the difference between unfolded protein at 70 °C and native at −15 °C and the absorbance change for the model compound over the same temperature range at 6 times the concentration of the protein. The concentration difference accounts for the tyrosine content of the protein. The amplitudes obtained for each set of conditions are similar to those obtained from the guanidine unfolding.

Double-Jump Unfolding Assay. The double-jump unfolding assay procedure of Schmid (1983) was modified for use with cryosolvent systems. The procedure was as follows. A 50-μL aliquot of 0.83 mM RNAse, 35% methanol, pH* 3.0, and 0.033 M sodium formate (or pH* 6.0 sodium acetate) was unfolded by incubation at 70 °C for 10 min in a glass syringe. We have previously shown by NMR that the protein is apparently unfolded under these conditions (Biringer & Fink, 1982a). This temperature is also above the A_{286}-observed unfolding transition. The solution was then injected into 200 μL of the same buffer at −15 °C. The maximum temperature during the transient rise in temperature on mixing was −7 °C. Since the rate of formation and breakdown of the slow-unfolding intermediate (I_2) is relatively slow, this brief rise in temperature is unlikely to have much effect on the results. After folding had progressed for a particular time period, a 100-μL aliquot was taken and injected into a spectrophotometer cell containing 900 μL of aqueous 5.0 M guanidine hydrochloride, pH* 6.0, at 10 °C. The decrease in absorbance at 286 nm was monitored as a function of time. The kinetic data were analyzed with semilog plots. The entire procedure was repeated for each selected folding time. The resulting amplitudes were calculated as a percentage of the average amplitude obtained for the unfolding of native RNase.

Other methods were as described previously (Biringer & Fink, 1988).

Results

Thermal Unfolding Transition. The thermal denaturation of RNase A was followed by absorbance change at 286 nm in aqueous and 35% methanol solutions at both pH* 3.0 and pH* 6.0. Typical 35% methanol data is shown in Figure 1. The values for the T_m's, the temperature at which half of the protein is in the unfolded state, were 44 and 59 °C in aqueous solution at pH 3.0 and 6.0, respectively, and 38 and 48 °C in 35% methanol at pH* 3.0 and 6.0, respectively. The values represent an average of four experiments for 35% methanol and a single experiment for aqueous at both pH values. The smaller effect of pH in the presence of methanol is probably a reflection of the effect of methanol on the p*K* of carboxyl groups. The 35% methanol will raise the p*K* of the exposed side-chain carboxyls (which have a p*K* close to 3.5) by about 0.5. The effect will be to shift the pH-dependent unfolding transition to a correspondingly higher value. The cooperativity of the transition for a given pH is lower in 35% methanol than in aqueous solutions.

The average molar extinction coefficient (M^{-1} cm^{-1}) at 286 nm for the difference between U at 70 °C and N at −15 °C, extrapolated to −15 °C and determined from the thermal unfolding transition, was 3320 at pH* 3 and 2900 at pH* 6. The corresponding values, obtained directly at −15 °C by using guanidine hydrochloride for unfolding, were 3000 at pH* 3 and 3260 at pH* 6.

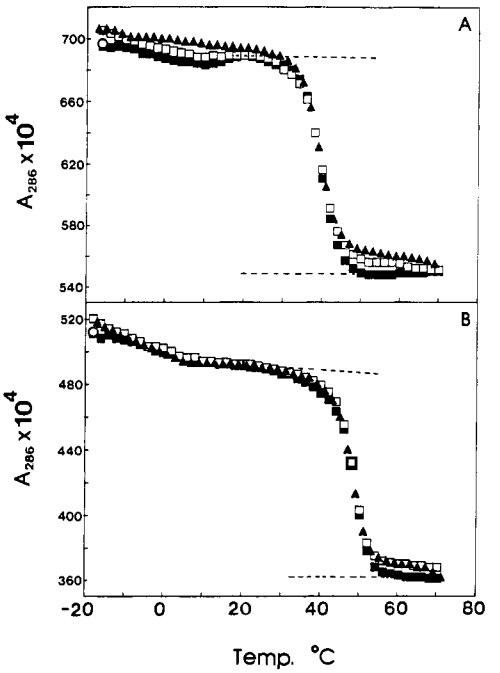

FIGURE 1: Sequential thermal folding/unfolding transitions of RNase A (7.1 μM) in 35% methanol as monitored by absorbance at 286 nm. Equilibrium *unfolding* is represented by (□) and subsequent *refolding* by (▲). The filled symbols represent those experiments that were performed first. The circle represents the final absorbance after the system was allowed to equilibrate at low temperature for several hours following the second unfolding/refolding cycle. (A) pH* 3.0, 0.033 M sodium formate; (B) pH* 6.0, 0.033 M sodium acetate.

Reversibility of Thermal Unfolding. Monitoring the equilibrium thermal unfolding/refolding transition by NMR indicated complete reversibility (Biringer & Fink, 1982a). The absorbance data for the thermal unfolding also indicated full reversibility, as the signal returned to its original value after the temperature was lowered and the system allowed to equilibrate for several hours (Figure 1). Some hysteresis was noted in experiments in which the enzyme was thermally unfolded, refolded, and then unfolded again. The hysteresis was only observed if the sample was initially heated to a temperature higher than the T_m. No change in p*I* was noted in IEF experiments of samples of RNase that had been thermally unfolded and refolded. It is likely that the hysteresis, in part, reflects the slow refolding at lower temperatures.

Refolding Kinetics Monitored by Absorbance. Each refolding experiment described in this section was performed under the following final conditions: 35% (v/v) methanol, −15.2 ± 0.2 °C, and pH* 3.0 or 6.0. The absorbance at 286 nm reflects the changes in exposure of tyrosine. In the native state, three of the six tyrosines are relatively exposed to solvent (Tyr-115, -76, -73) and three are relatively buried (Tyr-25, -92, -97).

When monitored by absorbance change, the folding process took 12×10^3 s for completion at pH* 3.0 and 6×10^3 s at pH* 6.0, under the experimental conditions used. Kinetic analysis indicated that four first-order transients were involved, each with a rate separated by about a factor of 5–10 from its neighbor (Table I). The plots in Figures 2 and 3 give the data in various stages of analysis. The top panel (A) in each gives a semilog plot for a sampling of the data representing the early portion of the folding with the observed data given in the inset. The middle panels (B) show the data after the slowest observed phase has been stripped from the data. The lower panels (C)

Table I: Kinetics of Refolding of Ribonuclease A at −15 °C, 35% Methanol[a]

	pH* 3.0				pH* 6.0			
signal	k_I(Amp)[b] × 10^2	k_{II}(Amp) × 10^2	k_{III}(Amp) × 10^3	k_{IV}(Amp) × 10^4	k_I × 10^2	k_{II}(Amp) × 10^2	k_{III}(Amp) × 10^3	k_{IV}(AMP) × 10^4
ΔA_{286}	6.2 ± 0.9 (dec)	1.3 ± 0.4 (19)	1.7 ± 0.4 (19)	2.9 ± 1.0 (19)	5.4 ± 1.2	1.0 ± 0.2 (−8)	3.3 ± 0.9 (9)	7.3 ± 1.0 (8)
fluorescence	ND	–	1.3 ± 0.4 (17)	3.0 ± 1.0 (7)	ND	–	1.7 ± 0.1 (19)	3.1 ± 0.3 (5)
115-NO_2	2.6 ± 0.6	0.88 ± 0.2 (37)	–	–	8.5 ± 1.0	1.6 ± 0.3 (26)	–	–
115,76-NO_2	2.3 ± 1.0	1.4 ± 0.2 (37)	0.82 ± 0.07 (9)	–	11.0 ± 2.0	1.6 ± 0.4 (12)	2.1 ± 0.6 (8)	–
115,76,73-NO_2	3.0 ± 0.7	0.8 ± 0.1 (26)	1.3 ± 0.4 (18)	–	4.0 ± 2.0	0.7 ± 0.06 (13)	1.5 ± 0.5 (10)	–
2′-CMP	–	2.1 ± 0.5 (9)	–	3.4 ± 0.8 (13)	–	1.8 ± 0.3 (19)	2.5 ± 0.3 (5)	–
2′,3′-CMP	ND	ND	3.2 (11)	2.4 (15)	–	ND	–	3.4 (23)
His C2[c]	ND	ND	2.6 (37)	–				

[a] The values in parentheses are the amplitudes of the given transient expressed as a percentage of the total amplitude change between U and N under the experimental conditions, from Biringer and Fink (1982b, 1988) and Biringer et al. (1988). [b] Rate constants are in units of s^{-1}, Amp = amplitude, ND means not determined, and (–) means the reaction was not observed. [c] Measured by proton NMR, from Biringer and Fink (1982b).

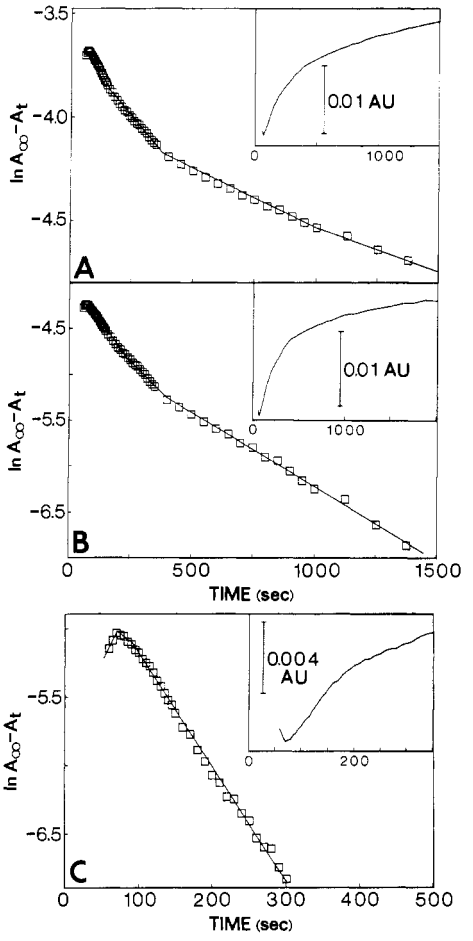

FIGURE 2: Time-dependent changes in the refolding of RNase A in 35% methanol, pH* 3.0, at −15 °C and 24 μM. Semilog plots are shown in order to emphasize the multiphasic nature of the refolding. The insets show the absorbance change at 286 nm as a function of time. One thousand data points were collected for the kinetic analysis. (A) A portion of the data showing the early phases of the refolding process; (B) the same data after the slowest phase was stripped out; (C) the data after the two slowest phases were factored out.

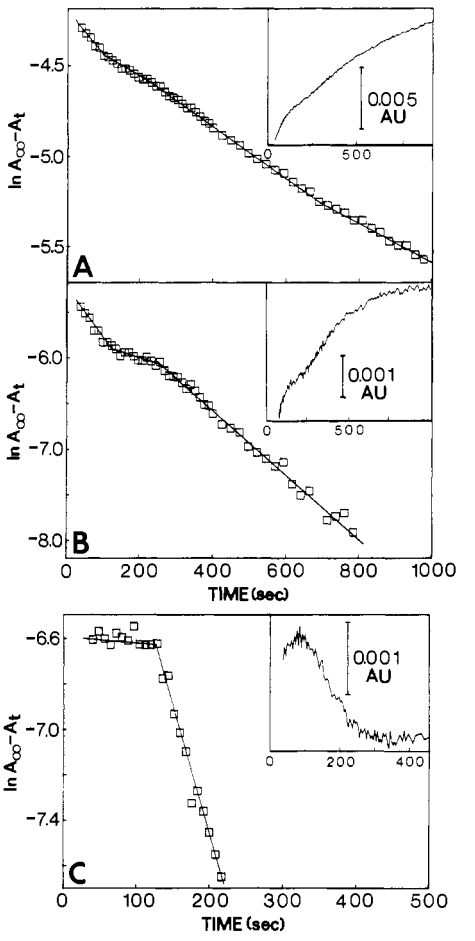

FIGURE 3: Time-dependent changes in the refolding of RNase A in 35% methanol, pH* 6.0, at −15 °C and 24 μM. Semilog plots are shown in order to emphasize the multiphasic nature of the refolding. The insets show the absorbance change at 286 nm as a function of time. One thousand data points were collected for the kinetic analysis. (A) A portion of the data showing the early phases of the refolding process; (B) the same data after the slowest phase was stripped out; (C) the data after the two slowest phases were factored out. Note that the "dip" seen around 200–400 s in panels A and B is due to the presence of a transient with a *decrease* in A_{286} (panel C, inset).

show the data after the two slowest processes have been stripped. The figures make it quite evident that the observed folding process consists of four distinct phases. The constraints imposed by the error introduced by multiple stripping do not allow precise measurement of the amplitudes of the fastest phase. The rate constants for this phase (k_I),[2] however, were quite reproducible.

The rates and amplitudes for the observed transients are given in Table I and represent an average of five experiments for pH* 3 and ten for pH* 6. The amplitudes are presented as a percentage of the amplitude difference between native and unfolded protein at −15 °C, in 35% methanol. Similar experiments were performed by using protein unfolded with Gdn·HCl. At pH* 6.0, the average rates and amplitudes (in parentheses) were 3.3×10^{-2} (20), 1.4×10^{-2} (−9), 4.5×10^{-3} (9), and 1.3×10^{-3} (7.5). These amplitudes are in excellent agreement with those for thermally unfolded protein (Table

[2] We will use the convention that *observed* rate constants will be indicated by roman numeral subscripts, whereas those for model schemes will be denoted by arabic subscripts.

Table II: Effect of pH* on Kinetics of Ribonuclease A Refolding[a]

pH*	signal[b]	k_1(Amp)[c] × 10^2	k_2(Amp) × 10^2	k_3(Amp) × 10^3	k_4(Amp) × 10^4
3.0	Abs	6.2 (−)[d]	1.3 (19)	1.7 (19)	2.9 (19)
4.0	Abs	*e*	2.9 (9.5)	1.2 (9.1)	3.6 (10.1)
5.0	Abs	1.0 (11)	0.6 (−17)	2.5 (10.4)	6.9 (12.5)
6.0	Abs	5.4	1.0 (−8)	3.3 (9)	7.3 (8)
2.0	Flu.			1.3 (17)	2.3 (7)

[a] Conditions were 35% methanol and −15 °C. [b] Abs = measured by ΔA_{286}, and Flu. = fluorescence emission change at 305 nm. [c] Amp = amplitude as a percent of total difference between native and unfolded protein. [d] Absorbance change was a decrease, i.e., a negative amplitude change. [e] Due to the "crossover" of the two faster transients this phase was not resolved.

I); except for the fastest phase, the rates are slightly faster for the Gdn·HCl-unfolded samples. This similarity indicates that the method of unfolding is not critical for the observed transients. This may not be true for faster transients reflecting earlier stages of refolding, since there is probably residual structure in the thermally unfolded material.

The refolding rates obtained at pH* 6.0 differ somewhat from those obtained for pH* 3.0. The slowest two phases are about twice as fast at pH* 6. The amplitudes differ considerably at each pH. The amplitudes for refolding at pH* 6.0 are almost exactly half of those for pH* 3.0. The transients with rate k_I at pH* 3, and k_{II} at pH* 6, are observed as *decreases* in absorbance, in contrast to all the other processes which are observed as increases in absorbance. The burial of Tyr residues is expected to result in an increase in A_{286}. The resulting "dip" in the ΔA_{286} vs time curves is readily apparent in the pH* 6 data (Figure 3C), and at the earliest times in the data at pH* 3, and were quite reproducible. The decreases in absorbance are much more marked in experiments at −20 °C and lower (unpublished results).

The effect of pH* on the refolding reaction was briefly investigated, since preliminary results indicated that some of the observed transients showed pH-dependent rates. The data for refolding at −15 °C in 35% methanol over the pH* 3–6 range are given in Table II. Each entry in the table is the average of the values for several experiments. As the pH increases, the fastest transient, observed as a *decrease* in absorbance, slows down and becomes the second fastest phase at pH* 5. Simultaneously, the transient that was second fastest at low pH increases in rate as the pH increases, thus becoming the fastest phase at pH* 5. Because the rates of these two processes cross as the pH* increases there is some mixing of observed rates and amplitudes, especially around pH* 4. The rate of the slowest phase increases slowly with increasing pH*, suggesting that it does not reflect proline isomerization.

Refolding Monitored by Fluorescence. The folding of RNase A was monitored by fluorescence under the same sets of conditions as above. Folding is accompanied by a decrease in fluorescence. Typical data sets for pH* 3.0 and 6.0 are presented in Figure 4. When this probe is used, the folding process appears biphasic under each set of conditions. The rates and amplitudes are given in Table I. The amplitudes are reported as a percentage of the difference in fluorescence between Gdn·HCl-unfolded protein and native protein. These data differ significantly from those obtained from absorbance experiments in that both the rates and amplitudes are vitually pH independent. Furthermore, only the slowest two processes seen with ΔA_{286} are detected by fluorescence, and only 24% of the total expected fluorescence change is observed. The rates and amplitudes of the transients observed by fluorescence were independent of pH from pH* 2 to 6 [the rates at pH* 2 were 1.3×10^{-3} and 2.3×10^{-4}, respectively; the amplitudes were the same as for pH* 3.0 (Table I)].

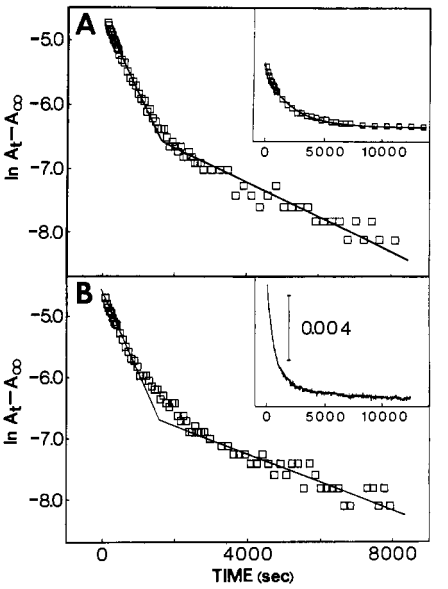

FIGURE 4: Time-dependent changes in the refolding of RNase A in 35% methanol, as monitored by fluorescence (excitation = 280 nm, emission = 305 nm), at [RNase] = 20.5 μM and −15 °C. Semilog plots of the amplitude of the fluorescence emission are shown with a sampling of data points. The insets show the change in fluorescence emission as a function of time. The units correspond to volts. (A) Data for pH* 3.0; (B) data for pH* 6.0. In the inset to panel A the solid line represents data from experiments using protein unfolded in 5 M Gdn·HCl; the open squares represent data using thermally unfolded protein.

Methanol-Induced Structure. Since methanol will have a higher affinity for hydrophobic groups and a lower affinity for polar groups than water, it might induce structure that is not present in aqueous solutions. In addition, alcohols have long been known to potentially induce additional structure in proteins (Tanford, 1970). In the folding process one must also be concerned with the structure of intermediate states which may be more sensitive to solvent. The model compound selected to study this possibility was carboxymethylated, reduced RNase A. This derivative is formed by reductive alkylation of all cysteine residues, which results in the irreversible cleavage of the four disulfide linkages. Studies have shown (Takahashi et al., 1977) that the resulting product has relatively little secondary structure. If methanol induces structure in partially folded RNase A, it should also do so in the carboxymethylated, reduced derivative.

A refolding experiment was thus performed with this derivative. The folding conditions were pH* 3.0, 10.5 μM, protein, and −15 °C. The absorbance of the sample was monitored at 286 nm, and the resulting trace is shown in Figure 5 along with a trace from a folding experiment with unmodified protein. The absence of time-dependent changes in absorbance for the reduced–alkylated derivative indicates that the presence of methanol does not induce significant structure under the experimental conditions. This was confirmed by carrying out the experiment in the reverse direction, namely, by unfolding the protein. In separate experiments, both RNase A and the derivative were incubated in 35% methanol, pH* 3.0 (0.033 M sodium formate), at room temperature and then injected into 5.0 M aqueous guanidine hydrochloride, pH* 6.0, at 10.0 °C. The final concentrations were 10.5 μM protein, 4.8 M guanidine hydrochloride, and 1.1% methanol. The resulting kinetic traces are given in Figure 5B. Only the RNase A showed any change in absorbance. The results of the two sets of experiments strongly suggest that

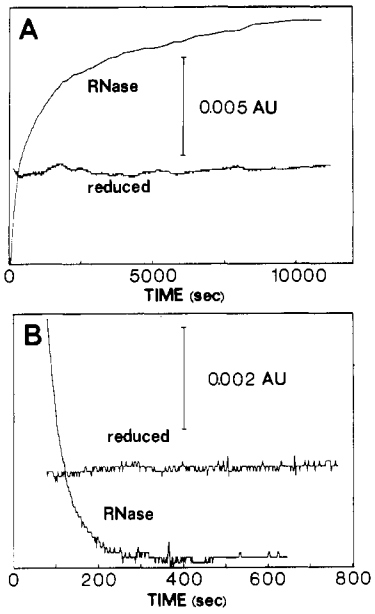

FIGURE 5: Time-dependent changes in the refolding and unfolding of both RNase A and carboxymethylated RNase A: (A) refolding of RNase A (corrected to 10.6 μM) and carboxymethylated RNase, 10.6 μM, −15 °C, pH* 3.0; (B) unfolding of RNase A and carboxymethylated RNase in 4.8 M guanidine hydrochloride, 10.6 μM, pH* 6.0, 10 °C, 1.1% methanol. In each case, the proteins were incubated in 35% methanol, pH* 3.0, prior to unfolding.

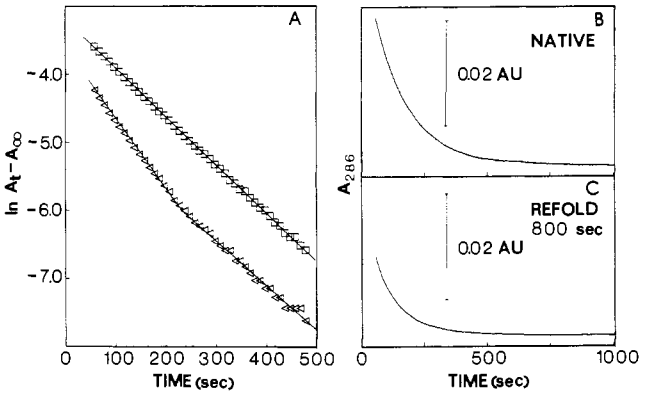

FIGURE 6: Double-jump unfolding assay of ribonuclease A refolding at pH* 3.0, in 35% methanol, −15 °C: (A) semilog plots of unfolding after 800 s of refolding (lower curve) and after complete refolding (upper line); (B) observed decrease in A_{286} during unfolding assay after completion of refolding; (C) as in (B) but after 800 s of refolding.

neither methanol nor low temperature induces artificial structure in either polypeptide, under these experimental conditions.[3] This was confirmed by deconvolution of circular dichroism spectra of native RNase in 50% methanol, pH* 3.0, which indicates identical amounts of secondary structure to that of the native state in aqueous solution (A. L. Fink and B. Lustig, unpublished observations).

Double-Jump Unfolding Assays. Ribonuclease A was allowed to refold for various time periods at −15 °C before being unfolded under similar conditions to those used by Schmid (1983), namely, 4.5 M Gdn·HCl, pH 6.0, and 10 °C. The unfolding was clearly biphasic during the first several thousand seconds, which is consistent with the unfolding of an intermediate state at a faster rate than the native state. The results

[3] We have observed, with far-UV circular dichroism, that significant secondary structure can be detected in reduced, alkylated ribonuclease in the presence of methanol under some conditions of pH and temperature.

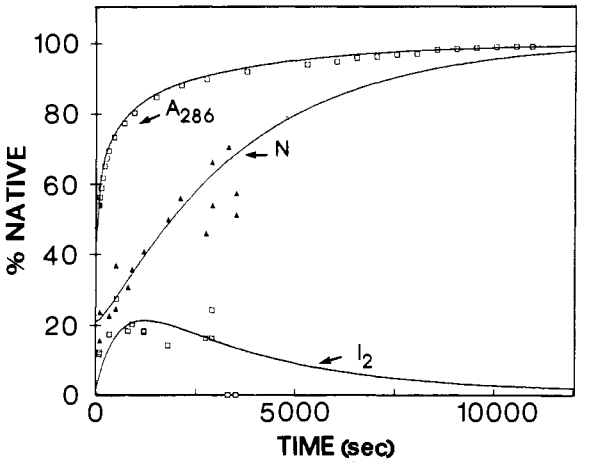

FIGURE 7: Results of double-jump unfolding assays and simulations of the model of Scheme I, at pH* 3.0. The solid curves were fitted with the data shown in Table III. The lower curve corresponds to the buildup of the intermediate (I_2) detected in the unfolding assays. The solid triangles represent the concentration of native state (N), as determined by the unfolding assays. The open squares represents data from the refolding reaction monitored by ΔA_{286}. Conditions were 35% methanol, −15 °C, and pH* 3.0. The ordinate represents the percentage of the total protein present.

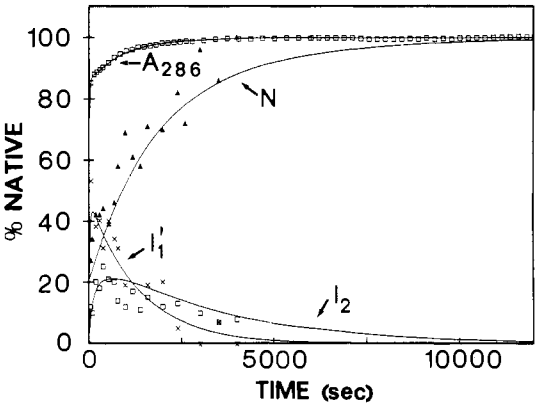

FIGURE 8: Results of double-jump unfolding assays and simulations of the model of Scheme I, at pH* 6.0. The solid curves were fitted with the data shown in Table III. The lower curve corresponds to the buildup of the intermediate (I_2) detected in the unfolding assays. The solid triangles represent the concentration of native state (N), as determined by the unfolding assays. The open squares represent data from the refolding reaction monitored by ΔA_{286}. The crosses represent the fast-unfolding intermediate, I'_1, of Scheme I. Conditions were 35% methanol, −15 °C, and pH* 6.0. The ordinate represents the percentage of the total protein present.

Table III: Kinetic Parameters for Species Observed in the Double-Jump Unfolding Assays and Simulations of the Absorbance Change at 286 nm during Refolding at −15 °C, in 35% Methanol[a]

	pH* 3.0	pH* 6.0		pH* 3.0	pH* 6.0
k_1	1.0×10^{-2}	1.0×10^{-2}	k'_1	1.2×10^{-2}	4.0×10^{-2}
k_2	1.7×10^{-3}	2.0×10^{-3}	k'_2	2.9×10^{-4}	7.5×10^{-4}
k_3	2.9×10^{-4}	3.0×10^{-4}			

[a] These data were used to generate the simulated curves shown in Figures 7 and 8. The parameters correspond to those in Scheme I. The rate constants are in s^{-1}.

of a typical unfolding assay are shown in Figure 6. From the amplitudes of the slow and fast phases it was possible to plot the time dependence of the buildup and decay of the observed intermediate (Figures 7 and 8). Similar data were obtained at both pH* 3.0 and pH* 6.0. The solid lines in Figures 7 and 8 were calculated with the parameters shown in Table III.

If the sum of the concentrations of fast-refolding material, intermediate, and native states is subtracted from 100%, the

resulting curve approaches 100% with a rate of 3×10^{-4} s^{-1}. However, this sum of concentrations lags substantially behind the change in ΔA_{286}, especially in the first third of the refolding reaction. This implies a second, parallel pathway to that containing the observed intermediate. Calculations from the data of Figures 7 and 8 indicate that approximately 50% of the unfolded state passes along this faster route to the native state.

Since this material does not show up in the unfolding assays, it must either be unfolded or be in the form of an intermediate (or intermediates) that unfolds (unfold) rapidly compared to the observed intermediate and native enzyme. On the basis of the change in ΔA_{286} in refolding, the material must be mostly, if not entirely, in the form of an intermediate (or intermediates) that unfolds (unfold) too rapidly to show up in the unfolding assays. The formation and decay of this intermediate (I'_1) is shown in Figure 8, and the kinetics of these processes are given in Table III (k'_1, k'_2). Confirmation of the presence of the second "invisible" folding pathway comes from experiments simulating the data for the unfolding assays and the observed changes in A_{286}.

Computer Simulations of Refolding. The simulations involved fitting the results for the double-jump unfolding assays, i.e., time-dependent changes in the concentration of intermediate and native state, and the data for refolding as monitored by ΔA_{286}. Simulations involving three consecutive processes or converging paths with one common intermediate could not be made to fit the data under any set of conditions. Only models involving two parallel pathways, each of which had an intermediate on it with absorbance properties similar to those of the native state, would fit both sets of data. Furthermore, it was necessary to assume the existence of an intermediate (I_1) preceding that observed in the double-jump assays on the minor pathway. In addition, the distribution of unfolded material between the two pathways of slow-refolding protein had to be in the 30% and 50% range. The data used to simulate the curves shown in Figures 7 and 8 are given in Table III.

The results indicate that in 35% methanol at −15 °C there are two parallel pathways for slow-folding material; the minor pathway consists of 30% of the refolding protein with a rate-limiting step of 3×10^{-4} s^{-1}, and the major pathway consits of 50% of the refolding protein with rate-limiting steps of 3×10^{-4} (pH* 2.9) and 7.5×10^{-4} (pH* 6.0) s^{-1}. Scheme I summarizes the minimum folding mechanism that is consistent with the double-jump unfolding assays. I_2 represents the intermediate directly observed in the double-jump assays.

Scheme I

$$U_F \rightarrow N \qquad (20\%)$$

$$U_S^I \xrightarrow{k_1} I_1 \xrightarrow{k_2} I_2 \xrightarrow{k_3} N \qquad (30\%)$$

$$U_S^{II} \xrightarrow{k'_1} I'_1 \xrightarrow{k'_2} N \qquad (50\%)$$

As shown in Table III there is no appreciable pH dependence for the steps in the minor slow-refolding pathway; however, the rates for the intermediate conversions in the major pathway are both pH-dependent, although to different extents.

In order to arrive at a detailed model for the folding of RNase in 35% methanol at −15 °C, the results from the double-jump unfolding assays were combined with those from experiments monitoring the kinetics of refolding reported above and in the preceding papers (Biringer & Fink, 1988; Biringer et al., 1988), using a variety of different probes. For convenience, the kinetic data have been summarized in Table I.

Discussion

Reversible Thermal Unfolding. The thermal transition in aqueous methanol is somewhat less cooperative than in aqueous solution (Fink & Painter, 1987). A possible pretransition zone can be observed in the 10–30 °C region at pH* 3 and in the 5–35 °C region at pH* 6 (panels A and B, respectively, of Figure 1). A small but significant amount of hysteresis was observed in the thermal unfolding/refolding curves. The effect is most pronounced in the 35% methanol data obtained at pH* 3 (Figure 1A). The final absorbance obtained after the second thermal refolding shows that the process is completely reversible. This, and the isoelectric focusing controls, rules out the possibility that deamidation (or other likely covalent modifications) is responsible for the hysteresis.

Fast- and Slow-Refolding Species. Baldwin and co-workers [e.g., Garel et al. (1975), Hagerman and Baldwin (1976), Nall et al. (1978), and Hagerman et al. (1979)] have shown that unfolded RNase A exists as an equilibrium mixture between two different forms, U_S and U_F, in which U_F refolds rapidly whereas U_S refolds slowly. For thermally unfolded RNase A, in aqueous solution at pH 3, the ratio of U_F to U_S is 1:4, i.e., 80% slow folding (Garel & Baldwin, 1975). The results of the double-jump unfolding assays show that a similar ratio of U_F/U_S is found when unfolding is carried out at pH* 3 in 35% methanol (see below) and also that refolding in cryosolvent is independent of the pH* of unfolding (between 3 and 6). Thus 20% of the refolding amplitude in the present study will be regained too fast to be observed, corresponding to the reaction:

$$U_F \rightarrow N \qquad (20\%)$$

In aqueous solution there are two significant forms of the slow-folding state of RNase A, U_S^I and U_S^{II}, with some evidence for a third form in amounts of 5% or less (Lin & Brandts, 1983a–c, 1984; Schmid, 1981; Schmid & Blaschеck, 1981; Mui et al., 1985). It was initially proposed by Brandts et al. (1975) that the slow-refolding forms of RNase A were due to the presence of the nonnative trans conformation of Pro-93 and Pro-114. In the native state prolines-93 and -114 are in the cis conformation. Subsequent investigations have cast some doubt upon proline isomerization being the source of the major slow-folding species. Using isomer-specific proteolysis, Lin and Brandts (1983a,b) showed that only 30% of the slow-refolding material has Pro-93 in the incorrect conformation. During refolding the rate of isomerization of Pro-93 corresponded to the rate of return of 30% catalytic activity. Their absorbance and fluorescence spectroscopic studies were consistent with a minor slow-refolding state, ascribed to process CT (30%) and corresponding to the isomerization of Pro-93, and a major slow-refolding species, corresponding to a process XY (50%) of unknown origin, as well as the 20% fast-refolding material (Lin & Brandts, 1983b).

It has also been suggested, however, that Pro-93 isomerization may be involved in both slow-folding pathways (Krebs et al., 1985; Schmid et al., 1986) [see also Schmid and Baldwin (1979), Schmid (1982, 1983), and Mui et al. (1985)]. In aqueous solution it has been shown that there are differences in the fluorescence properties of U_S and U_F (Schmid, 1981), whereas the absorbance properties are indistinguishable. In refolding, two phases are observed for the slow-folding material (corresponding to U_S^I and U_S^{II}). Under native-like refolding conditions absorbance measurements show two major transients, the faster having an amplitude of 50% of the total change (Lin & Brandts, 1983c; Mui et al., 1985); with fluorescence detection this phase corresponds to 35% of the total amplitude change; i.e., the major slow-refolding phases

observed by absorbance corresponds to the minor slow-refolding phase when observed by fluorescence in aqueous solution. In aqueous solution under strongly native conditions of refolding the slower transient observed by absorbance is faster than that observed by fluoresence, whereas under marginally native conditions both signals show the same rate.

Kinetics of Refolding: *Fluorescence*. Schmid (1981; Rehage & Schmid, 1982; Krebs et al., 1985; Schmid et al., 1986), Lin and Brandts (1983b), and Mui et al. (1985) have shown that the fluorescence change associated with the slowest folding step in RNase A refolding in aqueous solution reflects the isomerization of Pro-93, which is adjacent to Tyr-92. This is a reflection of the fact that the main source of the fluorescence change on folding comes from Tyr-92. Since a transient with a rate corresponding to the transient with rate k_{IV} observed with fluorescence is not seen in the absorbance experiments with the nitrotyrosine derivatives (Biringer & Fink, 1988), we can conclude that its source must be one of the remaining tyrosine residues, namely, Tyr-25, -92, or -97. Hence we attribute the slowest phase observed with fluorescence monitoring at subzero temperatures to a signal from Tyr-92. Given the small amplitude of the slowest phase observed by fluorescence (k_{IV}), its pH independence, and analogy with the aqueous case, we assign this step to the isomerization of Pro-93. The ratio of amplitudes observed in the present case is similar to that seen by Schmid and Blascheck (1981) when RNase A is refolded under strongly native conditions in aqueous solution, in which the slowest phase was shown to parallel the rate of proline isomerization.

The double-jump, unfolding assays indicate that about 30% of the protein refolds along one pathway under our experimental conditions and about 50% along a second pathway. The observed fluorescence amplitude changes in the present study, 24% of the total, correspond closely to the amount expected for the minor pathway. In addition, coupling between two processes with rates corresponding to k_{III} and k_{IV} was observed in the double-jump unfolding assays at both pH* 3 and pH* 6. Thus we attribute the fluorescence changes observed in unfolding (Figure 4) to the minor slow-refolding pathway. An alternative interpretation which cannot be excluded is that both transients observed by fluorescence correspond to the isomerization of Pro-93. The rates are different due to local environmental effects during the folding process (Schmid, 1986). The reason for there then being two slow-refolding paths may reside in the existence of Pro-114 in the nonnative conformation in the molecules on the minor pathway as well. Pro-114 could isomerize much more rapidly due to its different environment during folding.

Kinetics of Refolding: *Absorbance*. The changes in absorbance at 286 nm emanate from the six tyrosine residues in the protein, presumably with nonuniform contributions from individual residues due to differences in their local environments. For example, the three most buried residues, Tyr-92, -97, and -25, would be expected to contribute significantly more to the observed changes between native and unfolded protein than the more exposed Tyr-73, -76, and -115. Consequently, it is difficult to use changes in A_{286} to determine specific details about the refolding process. Furthermore, direct comparison of amplitudes with the reaction monitored by absorbance in aqueous solution is not possible due to *solvent* effects on the exposed Tyr residues.

The fastest process seen at pH* 3 (k_I) and the second fastest at pH* 6 (k_{II}) both showed *decreases* in absorbance! This reaction is much more evident at lower temperatures, especially at pH* 6 (R. G. Biringer, B. Lustig, and A. L. Fink, unpublished observations). The decrease in ΔA_{286} is a very interesting observation. Formally, since the refolding involves the burial of solvent-exposed Tyr residues and a concomitant increase in absorbance, this decrease implies an unfolding process or at least the exposure to a polar environment of a previously buried tyrosine.

One possible explanation for the absorbance decrease is that on injection of the unfolded protein into the native refolding conditions hydrophobic clusters are very rapidly formed in which the nonpolar side chains are buried. The refolding pathway to native protein then effectively begins from a state in which the tyrosine residues may not be solvent exposed. Such an interpretation, however, is inconsistent with our observations and can be discounted. The most probable source of the decrease in absorbance at 286 nm is that folding involves a transient partially folded state in which a tyrosine residue is more buried than in the final native state. Transformation to subsequent intermediates with native-like environments leads to the observed decrease in A_{286}. The intermediate may or may not be on the productive folding pathway.

Unfolding Assays. The basis of these assays was the observation by Schmid (1982) that under appropriate conditions the rate of unfolding of native RNase is considerably slower than that of the native-like intermediate, I_N. The results presented in Figures 7 and 8 indicate that a similar situation exists when unfolding and refolding are carried out in the presence of methanol. Thus we can assume that a native-like intermediate (I_2 in Scheme I), similar to I_N, is formed during refolding in 35% methanol at subzero temperatures. Figures 7 and 8 also show that at very early times there is already 20% native material, thus confirming that under our *unfolding* conditions 20% of the unfolded state is in the fast-folding form, U_F.

The results of the double-jump assays thus indicate a minimum scheme of the sort shown in Scheme I. The disposition of unfolded states is similar to that observed in aqueous solution, as is the presence of a native-like intermediate that unfolds relatively slowly.

Refolding at Subzero Temperatures. There are a number of points that should be kept in mind regarding the results from the kinetics of refolding at subzero temperatures in aqueous methanol. First, although there are many similarities with the results from similar experiments in aqueous solution and it is therefore tempting to assume that similar phenomena are occurring, we wish to stress that at the present time the subzero temperature experiments should be considered only as a potential *model* for what occurs in aqueous solution. The observations we have made in the present study suggest that we are seeing events late in the folding process, certainly no earlier than collapse of secondary structure to form tertiary structure.

In addition some caveats regarding the use of thermally unfolded protein in refolding kinetics experiments should be stated. First, although proton NMR experiments suggest that our thermally unfolded protein has lost all regular structure, it is very likely that the protein retains some local structure and is not by any means a random coil. For example, it is quite possible that some residual secondary structure remains. Since we are observing events late in the folding process, this is not necessarily a problem, and the fact that we see similar results with Gdn·HCl-unfolded protein confirms this. The addition of the hot thermally unfolded protein sample to the cold cryosolvent solution allows the potential for some refolding to occur during the cooling and mixing process. Undoubtedly, some partial refolding may occur and might account for the slightly larger amplitudes observed in some of the refolding

experiments using Gdn·HCl-unfolded protein and for the substantial amount of protein that refolded into native or native-like states via the major (faster) slow-refolding pathway (see below). However, the results of the double-jump unfolding experiments indicate that no significant amount of refolding to native state occurred, as does the similarity in results observed with thermally and Gdn·HCl-unfolded protein (Biringer & Fink, 1988).

Refolding Kinetics from Other Experiments. Previous papers in this series (Biringer & Fink, 1988; Biringer et al., 1988) report the results of refolding experiments at −15 °C in which several different probes were used to monitor the kinetics of refolding. It is our purpose in the next two sections to combine these results, summarized in Table I, with those of the double-jump unfolding assays to produce a model for the folding pathway.

The Major Slow-Folding Pathway. Mostly on the basis of the magnitude of their amplitudes (25–35%), we assign the transients observed by 2′-CMP binding, return of catalytic activity, fluorescence, and NMR (His C2 protons) to the *minor* slow-folding pathway. The remainder are assigned to the major slow-refolding path. The fastest transient associated with the major pathway is that detected by the nitro-Tyr derivatives, with $k = 2.5 \times 10^{-2}$ s^{-1} at pH* 3, increasing fourfold to approximately 1×10^{-1} s^{-1} at pH* 6. Both the unfolding assays and the nitro-Tyr derivatives show a slower transient with $k \approx 1.2 \times 10^{-2}$ s^{-1} at pH* 3 and a considerably faster rate constant at pH* 6 assigned to this path. In addition, we believe that the first transient exhibiting an increase in ΔA_{286} also corresponds to this step. Its rate is 1.3×10^{-2} s^{-1} at pH* 3 and 5.4×10^{-2} s^{-1} at pH* 6. Note that in each case the rate at pH* 6 is 4 times that at pH* 3.

The slowest transient associated with this pathway has a rate of 3×10^{-4} s^{-1} at pH* 3 and 7×10^{-4} s^{-1} at pH* 6 and is observed in the unfolding assays and by ΔA_{286}. The model for the major pathway is summarized in Scheme II.

Scheme II

$$U_S^{II} \xrightarrow{k'_1} I'_1 \xrightarrow{k'_2} I'_2 \xrightarrow{k'_3} N \qquad (50\%)$$

$$U_S^{I} \xrightarrow{k_1} I_1 \xrightarrow{k_2} I_2 \xrightarrow{k_3} I_3 \xrightarrow{k_4} N \qquad (30\%)$$

A number of features of this pathway may be inferred from the properties of the observed transients. The main one is that I'_2 must be very native-like, based on the fact that it has essentially full catalytic and inhibitor binding activity and is native-like by NMR. It differs from the native state, however, by a process characterized by a small change in absorbance at 286 nm, and by the fact that it unfolds very rapidly in the unfolding assay, much more rapidly than native protein and faster than can be detected in the assay. The process which converts I'_2 into the native state is characterized by a very slow rate, which is almost identical with that ascribed to the isomerization of Pro-93 (see below). It is unlikely that this process is due to the isomerization of Pro-114 since there is no change associated with the spectral properties of the adjacent nitro-Tyr-115 for this step.

The source of this slow conversion of I'_2 to N is not apparent at this time. However, it seems unlikely to be the isomerization of Pro-93, since this transient is pH-dependent (Table II), a property not expected for proline isomerization. The intermediate must be separated from the native state by a large energy barrier in view of the slow rate of conversion to native and the much faster rate of intermediate unfolding compared to that of native in the unfolding assays. The existing isomer-specific proteolysis experiments (Lin & Brandts, 1983a–c, 1984) make it unlikely that this step corresponds to the isomerization of some other proline, although many of the properties of this step are consistent with those expected for proline isomerization. However, Schmid and co-workers (Grafl et al., 1986) have reported evidence, based on homologous ribonucleases, that both slow-refolding species may have Pro-93 in the incorrect trans conformation. As discussed above, it is possible that the faster of the observed fluorescence transients could correspond to the isomerization of Pro-93 on the major pathway. If this is the case, then an additional species is required in Scheme II between I'_2 and N. Recently, Scheraga and co-workers have suggested that the slow step in the folding of U_S^{II} in aqueous solution may be due to incorrect chirality of one or more disulfides (Mui et al., 1985). Interconversion between two isomeric conformations of disulfide-bonded loops has also been suggested by Nall et al. (1978). Another explanation which cannot entirely be ruled out is the presence of a cis peptide bond not involving proline.

The major slow-refolding pathway is thus marked by the relatively rapid formation of a compact, substantially native-like species, I'_1. The spectral properties of I'_1 suggest that about one third of the native environment is present in the vicinity of Tyr-76 and -115. Conversion of this species into I'_2 results in the full native-like environment of the nitrotyrosines and essentially full catalytic and inhibitor-binding activity.

The Minor Slow-Folding Pathway. In contrast to the major slow-folding pathway, in which there appears to be no change in the pathway between pH* 3 and pH* 6 other than the small increase in the rate for each step, the data for the minor pathway are most easily fit to a simple model only if it is assumed that the pH dependence of individual steps on the pathway of folding is different. For example, the faster phase observed in the return of catalytic activity at pH* 3 (k_{III}) apparently slows down to the same rate as the slower phase (k_{IV}) at pH* 6. We interpret this to mean that there are two steps involved; the slower is pH-independent, and the faster is pH-dependent. Some of the observed transients ascribed to the minor path were pH-independent, such as both phases observed by fluorescence. Transients that showed the same pH dependence (or independence) and similar rates (within a factor of 2) were assigned to the same process.

We will first consider the situation at pH* 6.0 where most of the investigations of ribonuclease A refolding in aqueous solution have been done. Several methods, namely, unfolding assays, ΔA_{286} (at pH* 3), fluorescence, and catalytic activity with 2′,3′-CMP, revealed a slowest transient with rate 3×10^{-4} s^{-1}. Similarly, several monitoring techniques indicated a transient with rate around 2×10^{-3} s^{-1}; these included unfolding assays, fluorescence, inhibitor binding, and nitro-Tyr-76 (Table I). Simulations revealed that the penultimate phase (k_{III}) observed by ΔA_{286} also corresponds to this step. The fastest transients attributed to this pathway have a rate around 1.5×10^{-2} s^{-1} and are detected by nitro-Tyr-115, nitro-Tyr-76, inhibitor binding, and ΔA_{286}. In each case the sum of the amplitudes corresponds to about 25% of the total expected for U to N, with the exception of ΔA_{286}, for which a 25–30% contribution was confirmed independently by simulations and the double-jump unfolding assay.

At pH* 3 the minor pathway begins with the transient observed as a decrease in ΔA_{286} with rate 6×10^{-2} s^{-1}. The next phase is detected by transients with rates in the region of $(1–2) \times 10^{-2}$ s^{-1}. Probes detecting these kinetic phases included inhibitor binding and nitro-Tyr-115 and -76. The subsequent stage involves transients with rates in the range

of (1–3) × 10^{-3} s^{-1}. On the basis of differences in their pH dependencies it is most likely that there are two different underlying steps represented by these latter transients. However, for simplicity we will consider them as reflecting a single stage. This step is observed by unfolding assay, absorbance, fluorescence, catalytic activity, and His C2 protons (NMR) and corresponds to the formation of an intermediate (I_3) with native-like properties. The slowest observed phase has a rate of 3 × 10^{-4} s^{-1} and is detected by fluorescence, inhibitor binding, and catalytic activity.

The minimum scheme to represent folding by the minor pathway is given by Scheme II. As in the case of the major pathway, we can infer structural details about the intermediate states on the minor slow-folding path. On the basis of the NMR changes in His C2 protons (Biringer & Fink, 1982b) we can say that I_2 is significantly unfolded but also relatively compact, since the chemical shifts of the His protons are substantially shifted from their position in the fully unfolded state and yet still far from their positions in the native state. In addition, the relationship of the chemical shifts of the resonances is different from that in the native state. The NMR data indicate that I_3 is native-like as far as its His residues are concerned. We interpret this to mean that the basic three-dimensional structure of I_3 is very similar to that of the native state. Thus, whatever the difference between I_3 and N, it is not a gross structural one.

As discussed previously, we attribute the slowest step, involving the conversion of I_3 (analogous to I_N in aqueous solution) to N, to the isomerization of Pro-93. It is in this last phase at both pH* 3 and pH* 6 that the full catalytic activity returns. By all the other criteria we have used to investigate the refolding reaction, the preceding intermediate (I_3) is native-like.

On the basis of the nitro-Tyr-115 results we conclude that I_2 is native-like in the region of Tyr-115. However, from the data for nitro-Tyr-76, the region in the vicinity of Tyr-76 is not yet in its native environment in these intermediates. Interestingly, I_3, the native-like intermediate at pH* 3, shows partial catalytic activity (approximately one-third that of the native state), whereas the corresponding species at pH* 6 is essentially catalytically inactive. This apparent anomaly may just be a reflection of the lumping of several distinct intermediate states together in our attempt to keep the model simple. However, it is clear that at pH* 3 there is a partially folded, relatively native-like species which has some catalytic activity.

The results of the refolding with 2′-CMP at pH* 6 reveal the presence of intermediates that have inhibitor-binding activity but no catalytic activity. Thus I_2 has partial (approximately 75%) inhibitor-binding activity. The remainder of the inhibitor binding activity is present in I_3, which lacks *catalytic* activity. This means that the region of the molecule involved in binding the nucleotide must be intact in I_2. It is possible that the lack of catalytic activity reflects the absence of the N-terminal helix (the S-peptide region) from its native position in the cleft where it supplies the imidazole of His-12 which is required for catalysis. Alternately, since the activity returns in the step associated with the isomerization of Pro-93, the absence of activity may reflect the lack of correct positioning of other essential catalytic groups due to small deviations from the native state. In fact, the loop containing Pro-93 is spatially close to the backbone in the vicinity of Lys-41 due to a disulfide bond (Cys-95–Cys-40) and hydrogen bonds from the side chains of Tyr-92 and -97. One would expect the catalytic activity to be very sensitive to small distortions in the active site, so this latter interpretation is probably the correct one.

The observed transients clearly correspond to stages fairly late in the folding process and can be assumed to represent relatively discrete pathways with reasonably well-defined intermediate states, as indicated in Scheme II. However, we assume that there will be numerous conformations present in the earlier stages of the folding process.

Comparison with Refolding in Aqueous Solution. Investigations in aqueous solution have shown that the refolding of ribonuclease A is complex. The results from our studies at subzero temperatures in 35% methanol using multiple environment-sensitive probes at different pH values indicate even greater complexity. Some of this additional complexity stems from the experimental conditions and some from the wider variety of probes used to monitor the reaction. Although the minor refolding pathway in aqueous solution has not been investigated in much detail, nor have there been many investigations at pH <5, there have been reports of the presence of an intermediate formed early in the folding process (Schmid & Baldwin, 1979), as well as the relatively well characterized N-like intermediate. As in the case for refolding in aqueous solutions, we observe three main pathways of refolding (Scheme I). Since both the amplitude of the observed intermediate in the double-jump unfolding assays (Schmid, 1983) and the UV absorbance changes associated with refolding (Schmid, 1981; Lin & Brandts, 1983b) are very dependent on the experimental conditions used for the refolding, direct comparisons of these parameters cannot be made for folding in aqueous and cryosolvent systems.

In addition, different spectroscopic properties are expected for the various states in the cryosolvent as compared to aqueous solution, due to the exposure of the aromatic side chains to the less polar methanol and consequent solvent effects on the excited states. However, there is no obvious inconsistency in the overall properties of the folding process in the two solvent systems. Thus it seems reasonable that the factors which determine the folding pathway in aqueous solution are also in effect in the cryosolvent system. Therefore, the cryosolvent system serves as a model for the folding pathway in aqueous solution.

Mechanism of Protein Folding. Our observations are consistent with the following picture of protein folding: Initially, local regions of metastable units of structure, including secondary structural units, flicker back and forth with the unfolded state until their interactions result in the formation of more stable larger units of structure, probably through both hydrogen bonding and hydrophobic interactions. These units,in turn, pack with each other, predominantly through hydrophobic interactions due to the presence of exposed nonpolar residues on their surfaces. Eventually, sufficiently stable structural regions will form to result in the existence of discrete intermediate states, which will resemble the earliest detected or inferred states in this study. These states will then lead to a loosely packed, tertiary structure that undergoes final conformational rearrangements to give the native (or native-like)[4] state.

The ability to measure the rate at which a particular local region of the molecule attains its native environment could be used, if enough suitable probes were available, to map the pathway of folding in great detail. Comparison of the transients observed during refolding monitored by the different probes used in the present study demonstrates the potential

[4] In those instances where the last stage is the isomerization of a nonnative proline conformation.

of this approach and is a step toward the goal of mapping the folding pathway. In particular, methods such as nitration of tyrosine, NMR, circular dichroism, and other forms of chromophoric modification of individual residues, will undoubtedly play a much greater role in future studies of protein folding.

The present investigation indicates that cryosolvents and subzero temperatures may be used to substantially extend the opportunities for observing the folding process. The greater hydrophobicity of the cryosolvent, as compared to aqueous solution, will lead to stabilization of partially folded intermediates in which nonpolar groups are exposed to solvent. The extended temperature range for observation may result in much greater resolution of intermediates, due to substantial differences in activation energies for the different intermediate transformations.

Registry No. RNase, 9001-99-4; Pro, 147-85-3.

REFERENCES

Biringer, R. G., & Fink, A. L. (1982a) *J. Mol. Biol. 160*, 87–116.

Biringer, R. G., & Fink, A. L. (1982b) *Biochemistry 21*, 4748–4755.

Biringer, R. G., & Fink, A. L. (1988) *Biochemistry* (first of three papers in this issue).

Biringer, R. G., Austin, C. M., & Fink, A. L. (1988) *Biochemistry* (second of three papers in this issue).

Brandts, J. F., Halvorsen, H. R., & Brennan, M. (1975) *Biochemistry 14*, 4953–4963.

Cook, K. H., Schmid, F. X., & Baldwin, R. L. (1979) *Proc. Natl. Acad. Sci. U.S.A. 76*, 6157–6161.

Creighton, T. E., & Goldenberg, D. P. (1984) *J. Mol. Biol. 179*, 497–526.

Fink, A. L. (1986) *Methods Enzymol. 131*, 173–184.

Fink, A. L., & Painter, B. (1987) *Biochemistry 26*, 1665–1671.

Garel, J. R., & Baldwin, R. L. (1973) *Proc. Natl. Acad. Sci. U.S.A. 70*, 3347–3352.

Garel, J. R., & Baldwin, R. L. (1975) *J. Mol. Biol. 94*, 611–620.

Garel, J. R., Nall, B. T., & Baldwin, R. L. (1976) *Proc. Natl. Acad. Sci. U.S.A. 73*, 1853–1857.

Grafl, R., Lang, K., Wrba, A., & Schmid, F. X. (1986) *J. Mol. Biol. 191*, 281–293.

Hagerman, P. J., & Baldwin, R. L. (1976) *Biochemistry 15*, 1462–1473.

Hagerman, P. J., Schmid, F. X., & Baldwin, R. L. (1979) *Biochemistry 18*, 293–297.

Kim, P. S., & Baldwin, R. L. (1982) *Annu. Rev. Biochem. 51*, 459–489.

Krebs, H., Schmid, F. X., & Jaenicke, R. (1985) *Biochemistry 24*, 3846–3852.

Lin, L.-N., & Brandts, J. F. (1983a) *Biochemistry 22*, 559–563.

Lin, L.-N., & Brandts, J. F. (1983b) *Biochemistry 22*, 564–573.

Lin, L.-N., & Brandts, J. F. (1983c) *Biochemistry 22*, 573–580.

Lin, L.-N., & Brandts, J. F. (1984) *Biochemistry 23*, 5713–5723.

Mui, P. W., Konishi, Y., & Scheraga, H. A. (1985) *Biochemistry 24*, 4481–4489.

Nall, B. T., Garel, J., & Baldwin, R. L. (1978) *J. Mol. Biol. 118*, 317–330.

Rehage, A., & Schmid, F. X. (1982) *Biochemistry 21*, 1499–1505.

Schmid, F. X. (1981) *Eur. J. Biochem. 114*, 105–109.

Schmid, F. X. (1982) *Eur. J. Biochem. 128*, 77–80.

Schmid, F. X. (1983) *Biochemistry 22*, 4690–4696.

Schmid, F. X., & Baldwin, R. L. (1979) *J. Mol. Biol. 135*, 199–215.

Schmid, F. X., & Blaschek, H. A. (1981) *Eur. J. Biochem. 114*, 111–117.

Schmid, F. X., Grafl, R., Wrba, A., & Beintema, J. J. (1986) *Proc. Natl. Acad. Sci. U.S.A. 83*, 872–876.

Takahashi, S., Kontani, T., Yoneda, M., & Ooi, T. (1977) *J. Biochem. 82*, 1127–1133.

Tanford, C. (1970) *Adv. Protein Chem. 24*, 1–95.